Global Warming Determines Future Increase in Compound Dry and Hot Days within Wheat Growing Seasons Worldwide

Yan He
heyan01@foxmail.com
Chinese Academy of Meteorological Sciences
Yanxia Zhao
Chinese Academy of Meteorological Sciences https://orcid.org/0009-0000-6399-6464
Shao Sun
Chinese Academy of Meteorological Sciences
Jiayi Fang
Hangzhou Normal University
Yi Zhang
Chinese Academy of Meteorological Sciences
Qing Sun
Chinese Academy of Meteorological Sciences
Li Liu
Chinese Academy of Meteorological Sciences
Yihong Duan
Chinese Academy of Meteorological Sciences
Xiaokang Hu
Beijing Normal University
Peijun Shi
Beijing Normal University

Research Article

Keywords: Compound dry and hot days, Wheat growing season, Global breadbasket, Future, Climate extremes

Posted Date: August 23rd, 2023

DOI: https://doi.org/10.21203/rs.3.rs-3220211/v1

Additional Declarations:
References are available in Supplementary Files Section.

Declarations are available in Supplementary Files Section.

Version of Record: A version of this preprint was published at Climatic Change on April 10th, 2024. See the published version at https://doi.org/10.1007/s10584-024-03718-1.

Global Warming Determines Future Increase in Compound Dry and Hot Days within Wheat Growing Seasons Worldwide

Abstract

Compound drought and hot extremes are proved to be the most damaging climatic stressor to wheat production thereby with grave implications for global food security, thus it is critical to systematically reveal their future changes under unabated global warming. In this study, we comprehensively investigate the global changes of compound dry and hot days (CDHD) during dynamic wheat growing seasons of 2015-2100 under 4 socio-economic scenarios (SSP1-2.6, SSP2-4.5, SSP3-7.0 and SSP5-8.5) based on the latest downscaled Coupled Model Intercomparison Project Phase 6 (CMIP6) models. The results demonstrate a notable increase in CDHD's frequency ($CDHD_f$) and severity ($CDHD_s$) in the future, by the end of 21st century, global average $CDHD_f$ and $CDHD_s$ are expected to increase by 6.5~27.5 days and 0.43~1.43 with reference to 1995-2014. Adopting a low forcing pathway will reduce CDHD in up to 95.1% of wheat planting grids. As the top 10 wheat producer, Ukraine, Turkey and America will suffer much more and stronger CDHD in future wheat growing seasons under all SSPs. Global warming will dominate the future increase of CDHD worldwide directly by promoting hot days to increase and indirectly by enhancing potential evapotranspiration (PET) thereby promoting drought events. This study helps to optimize adaptation strategies for mitigating risks from CDHD on wheat production, and provides new insights and analysis paradigm for investigating future variations in compound extremes occurring within dynamic crops growing seasons worldwide.

Keywords: Compound dry and hot days; Wheat growing season; Global breadbasket; Future; Climate extremes

1 Introduction

Under global warming, the frequency and severity of climate extremes has increased disproportionally around the globe (IPCC, 2021), furthermore, it is proved that the relationship between climate extremes has been changed as well: the concurrence of climate extremes (also known as "compound extremes") are becoming more frequent (AghaKouchak et al., 2014; Zscheischler et al., 2018). Drought and hot extremes are two of the most detrimental climate extremes which can cause severe adverse impacts on ecosystem and society (Jia et al., 2022; Richardson et al., 2022). Nowadays, the concurrence of drought and hot extremes, also known as compound drought and hot extremes, have attracted raised attention because of their massive impacts that even larger than the sum of the impacts caused by individual drought or heat alone (Zscheischler et al., 2014). Despite the diversity of definitions and limitations of data, previous studies have demonstrated the substantial increase in compound drought and hot extremes, including their spatial extent, frequency and severity (Hao et al., 2013; Mazdiyasni et al., 2015; Manning et al., 2019; Wu et al., 2020). Given their amplified impacts on crops yield (Ribeiro et al., 2020; Li et al., 2022a), wildfires (Libonati et al., 2022), tree mortality (Gazol et al., 2022) and heat-related deaths (Mitchell et al., 2016), it is vital to sift the compound drought and hot extremes from individual droughts or heat, and systematically understand how they will change in the future.

Food security has been a major challenge as food supply need to increase by ~70% to meet demands at 2050s (Anon., 2009). However, food security is threatened seriously by drought and heat extremes associated with global warming (Lobell et al., 2013). Wheat is the first rainfed crop and the second irrigated crop after rice (Portmann et al., 2010), meanwhile, wheat is the most widely grown crop in the world with about 2.2 million km^2 total harvested area, and one of the most important cereal crops with great implication for global food security (Lobell et al., 2012). Wheat is highly sensitive to climate stresses, among of them, compound drought and hot extremes are proved to be the most damaging climate stressor for wheat production (Guerreiro et al., 2018), which has been identified as critical. The reasons are as follow. Firstly, drought and heat are typically triggered by similar synoptic circulation anomalies (Trenberth et al., 2005), thus leading to a significant correlation between them (Zscheischler et al., 2017b).

For instance, 2003 European heatwaves and 2010 Russia heatwaves were both accompanied by serious droughts (Ciais et al., 2005; Russo et al., 2015). Secondly, when drought and heat coincide, both of them will be intensified by local-and regional-scale land-atmosphere feedbacks (Miralles et al., 2019). Thirdly, the concurrent drought and heat stress have synergistic effects on wheat and then aggravate their adverse impacts (Suzuki et al., 2014). For instance, plant's vulnerability to high temperature will increase under drought condition, because drought will limit the plant's evaporative cooling thus reduce its's ability to regulate temperature (Neukam et al., 2016).

The past decade has witnessed considerable progress in investigating compound drought and hot extremes, including their causative mechanisms (Hao et al., 2018b), variations (Wang et al., 2020), related exposure (Liu et al., 2021; Zhang et al., 2022a; Wang et al., 2023) and impacts/risks (Ribeiro et al., 2020; Hao et al., 2021; Libonati et al., 2022). Recent studies have characterized compound drought and hot extremes by building compound indices based on both dry and hot conditions (Hao et al., 2018a; Hao et al., 2019; Feng et al., 2020a; Feng et al., 2020b; Wu et al., 2019) and the joint return periods based on copula analyses (AghaKouchak et al., 2014; Zscheischler et al., 2017b; Zscheischler et al., 2020). Nowadays, raised attention has been given to investigating compound drought and hot extremes related with crops growing, previous studies have been devoted to revealing their change characteristics during crops growing seasons and/or over crops planting regions (Feng et al., 2021; He et al., 2022a; Li et al., 2022b), and further, quantifying the impacts/risks on crops yield (Zscheischler et al., 2017a; Feng et al., 2019; Ribeiro et al., 2020; Luan et al., 2021; Li et al., 2022a). However, there is still a lack of systematic understanding for future changes in compound drought and hot extremes within crops' growing seasons, especially within dynamic crops' growing season, which is a vital and necessary cognition for food security risk reduction and climate change adaptation.

In this study, we focus on the compound dry and hot days (hereafter CDHD) occurring within wheat growing seasons worldwide, changes in frequency and severity of CDHD within dynamic wheat growing seasons of 2015-2100 are investigated over global wheat planting regions under different socio-economic scenarios. The objectives of this study are based on the following research questions: (a) How will the frequency and severity of CDHD within dynamic wheat growing seasons change in the future? What difference will adopting a low forcing pathway make for CDHD occurrence (section 3.1)? (b) For the Top 10 wheat producing countries, who will be the hotspots that facing more and stronger CDHD in wheat growing season (section 3.2)? (c) How will global warming dominate the increase of CDHD in the future (section 3.3)?

2 Data and methodology

2.1 Data

The latest version of the NASA Earth Exchange Global Daily Downscaled Projections (NEX-GDDP) is derived from the GCM simulations of CMIP6, which provides a set of high-resolution, bias-corrected climate change projections on global scale that can be used to investigate climate change impacts (Thrasher et al., 2022). In this study, we employ a multi-model ensemble containing 10 global climate models (GCMs) from NEX-GDDP (Table 1). Variables including daily precipitation, daily mean temperature and daily maximum temperature are available at 0.25° × 0.25° spatial resolution, covering historical (1950-2014) and future (2015-2100) under 4 different socio-economic scenarios: SSP1-2.6, SSP2-4.5, SSP3-7.0 and SSP5-8.5. Based on the CMIP6 ensemble median, these scenarios correspond to projected global warming magnitude of 2.2℃, 3.3℃, 4.3℃ and 5.1℃ at the end of 21 century respectively (Tabari et al., 2022). The period 1995-2014 is selected as the "reference period" because it is supposed to be the based period in IPCC sixth assessment report (IPCC AR6) (Tokarska et al., 2020). In addition, the two future periods, 2041-2060 and 2081-2100, are selected to represent "mid-term future" and "long-term future" respectively, which also underpin the IPCC AR6.

Table 1. Global climate models from CMIP6-NEX-GDDP used in this study

Model name	Institution with country	Temporal resolution	Spatial resolution
ACCESS-CM2	Commonwealth Scientific and Industrial Research Organization- Australian Research Council Centre of Excellence for Climate System Science (CSRO-ARCCSS), Australia	Daily	0.25° × 0.25°
CanESM5	Canadian Centre for Climate Modelling and		

	Analysis, Environment and Climate Change, Canada
CMCC-ESM2	Fondazione Centro Euro-Mediterraneo sui Cambiamenti Climatici (CMCC), Italy
EC-Earth3-Veg-LR	European Community Earth System Model, Europe
GFDL-ESM4	Geophysical Fluid Dynamics Laboratory, America
INM-CM4-8	Institute for Numerical Mathematics, Russian Academy of Science, Russia
IPSL-CM6A-LR	Institute Pierre Simon Laplace, France
MIROC6	Japan Agency for Marine-Earth Science and Technology, Japan
MPI-ESM1-2-LR	Max Planck Institute for Meteorology, Germany
NorESM2-MM	Norwegian Research Center, Norway

The global gridded land use dataset is projected by the Global Change Assessment Model (GCAM) and a land use spatial downscaling model (named Demeter), which provides the projections of planting area percentage for 32 plant functional types at 0.05° × 0.05° resolution over 2005–2100 (in 5 years-step length, 2005-2100) under 15 SSP-RCP scenarios (Chen et al., 2020). In this study, we use the projections of wheat planting area percentage (including rainfed wheat and irrigated wheat) under SSP1-RCP2.6, SSP2-RCP4.5, SSP3-RCP6.0 (no data relative to RCP7.0) and SSP5-RCP8.5 to match the climate variables projections under SSP1-2.6, SSP2-4.5, SSP3-7.0 and SSP5-8.5, respectively. To keep consistent with climate data, wheat planting area percentage data are aggregated from the original 0.05°resolution to 0.25° resolution, then the 0.25° grids with planting area percentage larger than 0 are identified as “wheat planting grids”. Since wheat planting area percentage is projected at 5-year resolution, we assume that the planting area percentage remain unchanged in each 5-year period, the wheat planting area percentage of a year represents the situation of the 5-year period that centering this year (for example, the wheat planting area percentage of 2020 represents the wheat planting area percentage during 2018-2022). Since this dataset does not distinguish winter wheat and spring wheat, the original distribution of winter/spring wheat is obtained from Crop Calendar

Dataset (Sacks et al., 2010) who providing the present distributions of winter/spring wheat at 5-min resolution. Based on the original winter/spring wheat distributions and the projections of rainfed/irrigated wheat mentioned above, the projections of the planting area of rainfed winter wheat, rainfed spring wheat, irrigated winter wheat and irrigated spring wheat are obtained, as shown in Fig. S1-S5.

GGCMI Phase 3 crop calendar is a composite product merging various observational data sources, providing static planting date and maturity date for 18 crops at 0.5° × 0.5° resolution. This crop calendar dataset separates rainfed and irrigated systems, and grid cells outside of currently cultivated areas are spatially extrapolated and original data gap-filled (Jagermeyr et al., 2021). In this study, GGCMI Phase 3 crop calendar provides the current planting date and maturity date for rainfed winter wheat, rainfed spring wheat, irrigated winter wheat and irrigated spring wheat at global scale (Fig. S6), which represents the current state of wheat growing season. To keep consistent with climate data, the crop calendar data are downscaled from the original 0.5°resolution to 0.25° resolution.

2.2 Methodology

2.2.1 Dynamic wheat growing season

In this study, we only focus on the CDHD that occurring within wheat growing seasons rather than the whole period, because these CDHD may cause adverse impacts on wheat. Some previous studies usually used a fixed crop calendar based on historical observations without considering the changes of crops growing seasons influenced by climate and anthropogenic factors thereby amplifying results' uncertainties. In this study, we try to improve wheat growing season from static to dynamic by considering the impacts of global warming on the length of wheat growing season. Although it should be noted that the changes in crop growing seasons are affected by both climate conditions and technological developments, this is initial and helpful exploration in the context of global warming.

Temperature can substantially affect wheat physiological processes thus control wheat phenology and the length of the required growing period (Wang et al., 2017). In this study, we define the dynamic wheat growing season via calculating the required time for wheat to reach maturity under the impacts of global warming, meanwhile, we assume that management strategies will keep consistent in the future-namely the planting dates and cultivar selection remain unchanged, according to Jagermeyr et al. (2021). The phenology scheme for wheat is adopted from LPJmL4 model, the phenological development of wheat is driven by temperature through the accumulation of heat units (HU) (Schaphoff et al., 2018). HU is accumulated daily, the daily HU increment (HU_i) is the difference between the daily mean temperature of day i ($T_{mean,i}$) and the base temperature (T_b, here is 0°C based on Schaphoff et al. (2018)), HU_i cannot be less than 0 at any given day (Eq. 1). The phenological heat units (PHU) is the sum of HU_i from planting date to maturity date, describing the total heat requirement over the growing season (Eq. 2) (Qiao et al., 2020). Based on the planting date and maturity date provided by GGCMI Phase 3 wheat crop calendar, the total heat requirement (THR) of a wheat planting grid is calculated as the average of PHU for the reference period 1995-2014 (Eq. 3):

$$HU_i = \begin{cases} 0 & T_{mean,i} \leq T_b \\ T_{mean,i} - T_b & T_{mean,i} > T_b \end{cases} \tag{1}$$

$$PHU = \sum_{i=planting\ date}^{i=maturity\ date} HU_i \tag{2}$$

$$THR = \frac{\sum_{y=1995}^{y=2014} PHU_y}{20} \tag{3}$$

For each wheat planting grid, the maturity date (MD) in each year of the future is the first day for HU accumulation to reach its total heat requirement calculated by Eq. 3. MD is calculated based on Eq. 4-5:

$$(\sum_{i=planting\ date}^{i=N} HU_i) \geq THR \tag{4}$$

$$MD = \min\{N\} \tag{5}$$

where N is the collection for HU accumulation reaching (or larger than) PHU_r, the maturity date MD is the minimum of N, that is, the first day for HU accumulation reaching THR. Based on this, we calculated the maturity date for each wheat planting grid and for each wheat growing season of 2015-2100 under 4 SSPs. The detailed changes in wheat growing season in the future are shown in Fig. S7-S8.

2.2.2 CDHD definition

In this study, a compound dry and hot day (CDHD) is defined as a hot day coincides with a drought event within a wheat growing season. Agricultural drought is a comprehensive phenomenon that comprising precipitation shortages, evapotranspiration reduction and soil moisture deficits (Łabędzki et al., 2015). The Standardized Precipitation Evapotranspiration Index (SPEI) is produced by standardizing the difference between water supply (precipitation) and demand (potential evapotranspiration, PET) (Vicente-Serrano et al., 2010), which is more sensitive to drought conditions due to the evaporative demand component, more robust in revealing droughts influenced by rising temperature in the context of global warming (Sein et al., 2021), and has higher correlation with crops yield (Tian et al., 2018). Here we calculate 1-month SPEI for each month during 1950-2100, a drought event is identified as monthly SPEI≤-1, based on this, we identify the drought events occurring within each wheat growing season of 2015-2100 in each wheat planting grid. PET is calculated based on Thornthwaite method (Thornthwaite 1948) (Eq. 6-8):

$$PET = 16K(\frac{10T}{I})^m \tag{6}$$

where K is a correction coefficient calculated as a function of the latitude and month; T is the mean monthly temperature (°C); I is the sum of the 12 monthly index values i according to Eq. 7, and m is a coefficient depending on I (Eq. 8)

$$i = (\frac{T}{5})^{1.514} \tag{7}$$

$$m = 6.75 \times 10^{-7} \times I^3 - 7.71 \times 10^{-5} \times I^2 + 1.79 \times 10^{-2} \times I + 0.492 \tag{8}$$

Heat stress is frequent during wheat growing season. Previous studies have proved that heat-shock above 30°C may change wheat growing season by shortening seed germination and maturity periods (Yamamoto et al., 2008), severely affect leaf development and production tiller formation (Ataur et al., 2009), and limit the dry matter accumulation in grain and even may cause complete sterility (Kaur et al., 2010). Thus in this study, daily maximum temperature ($Tmax$) greater than 30°C is set as the heat threshold, which is widely used for wheat in previous studies (Chen et al., 2016), accordingly, a hot day is defined as the $Tmax$ greater than 30°C. Based on this, we identify the hot days occurring within each wheat growing season of 2015-2100 in each wheat planting grid.

Based on the definition of drought event and hot day mentioned above, we identify all CDHD (hot days coincide with drought events) occurring within each wheat growing season of the reference period 1995-2014 and future period 2015-2100 (under SSP1-2.6, SSP2-4.5, SSP3-7.0 and SSP5-8.5) in each wheat planting grid. The methodology of CDHD identification is shown in Fig. 1.

Here we use the two indices, the frequency of CDHD ($CDHD_f$) and the severity of CDHD ($CDHD_s$), to characterize the future changes in CDHD. The $CDHD_f$ describe the frequency of CDHD occurring within a wheat growing season. The $CDHD_s$ is the average of the product of the daily SPEI value (daily SPEI value is as the same with this days' monthly SPEI value) and the daily standardized values of $Tmax$ for each CDHD, thereby $CDHD_s$ is given as:

$$CDHD_s = \frac{\sum_{i=1}^{CDHD_f}(-1 * SPEI_i) * (\frac{T_{max,i} - T_{high}}{T_{high} - T_{base}})}{CDHD_f} \quad (9)$$

where $CDHD_s$ is the severity of CDHD in a wheat growing season, $CDHD_f$ is the frequency of CDHD in this wheat growing season, $SPEI_i$ is the SPEI value of day i, $T_{max,i}$ is the daily maximum temperature of day i, T_{high} is the heat threshold (30℃ in this study), T_{base} is the base temperature representing the minimum biology temperature for wheat, here we use 5.5℃ according to existing studies (Zhu et al., 2018; He et al., 2022b). We calculate the $CDHD_f$ and $CDHD_s$ for each wheat growing season of the reference period 1995-2014 and future period 2015-2100 (under SSP1-2.6, SSP2-4.5, SSP3-7.0 and SSP5-8.5) in each wheat planting grid worldwide.

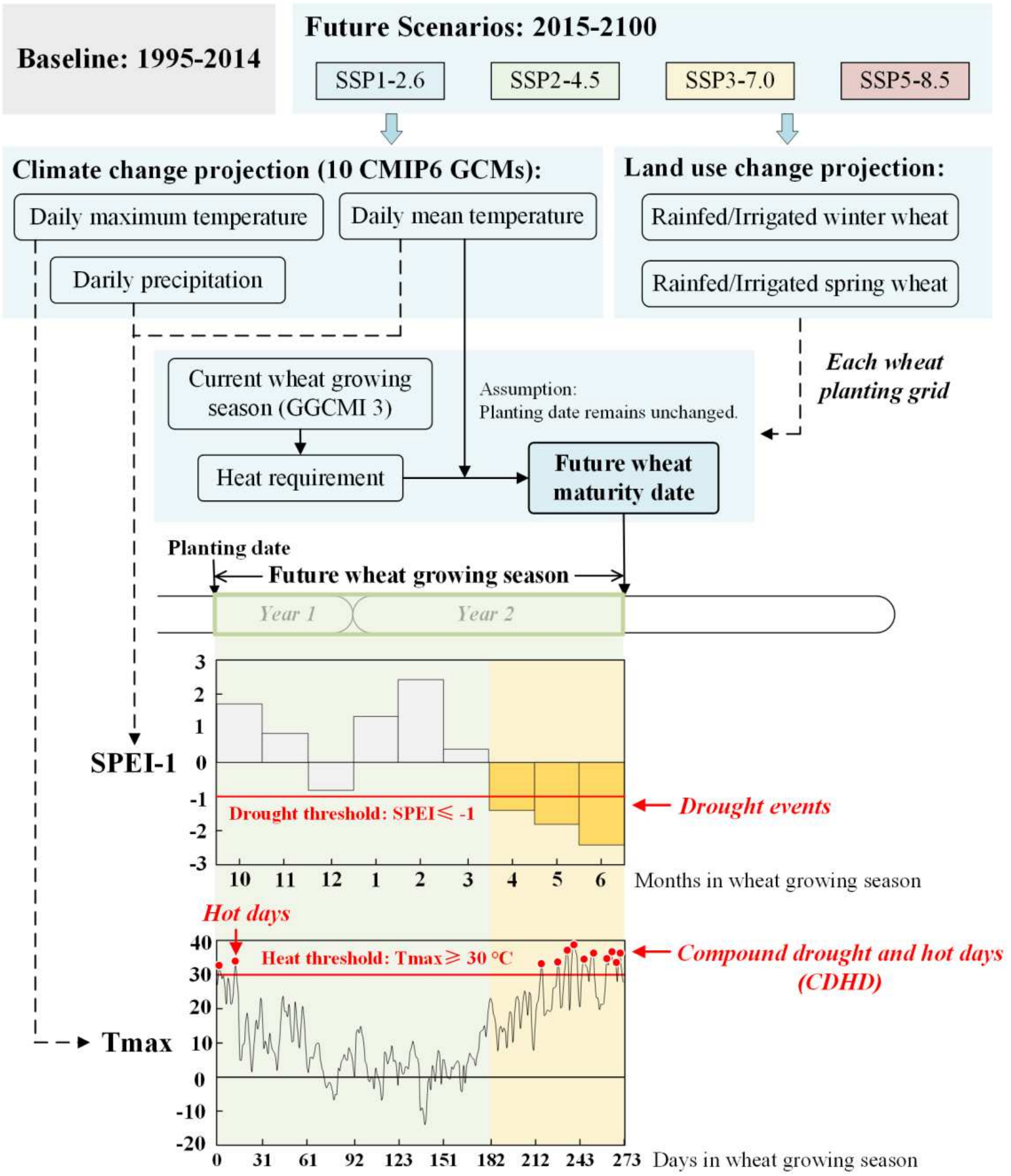

Fig. 1. Methodology of identifying CDHD in future wheat growing season.

3 Result

3.1 Future changes in CDHD within wheat growing seasons

Fig. 2 shows the global average changes in drought events, hot days, $CDHD_f$ and $CDHD_s$ for each wheat growing season during historical period (1951-2014) and future period (2015-2100). As Fig. 2(a) shows, drought events within wheat growing seasons will increase significantly during 2015-2100 under all 4 SSPs. Before ~2060s, the increased trends of drought events are similar among the 4 SSPs; after that, drought events turn to decrease under SSP1-

2.6, while continue to increase under SSP2-4.5, SSP3-7.0 and SSP5-8.5. The fastest increase will occur under SSP5-8.5, followed by SSP3-7.0 and SSP2-4.5. By 2100, drought events within a wheat growing season are projected to increase by 0.3 months, 0.8 months, 1.5 months and 1.7 months with reference to 1995-2014 under SSP1-2.6, SSP2-4.5, SSP3-7.0 and SSP5-8.5 respectively. As Fig. 2(b) shows, hot days within wheat growing seasons will increase significantly by 0.07d/y, 0.11d/y, 0.15d/y and 0.19d/y during 2015-2100 under SSP1-2.6, SSP2-4.5, SSP3-7.0 and SSP5-8.5 respectively. Hot days will keep increasing throughout the century, by 2100, hot days within a wheat growing season are projected to increase by 7.1 days, 11.2 days, 14.6 days and 17.4 days with reference to 1995-2014 under SSP1-2.6, SSP2-4.5, SSP3-7.0 and SSP5-8.5 respectively.

As Fig. 2(c) and Fig. 2(d) show, global average $CDHD_f$ and $CDHD_s$ are projected to increase significantly under all SSPs, indicating that wheat will suffer more and stronger CDHD during growth process in the future. Before ~2060s, the increased trends of $CDHD_f$ and $CDHD_s$ under the 4 SSPs are similar, which is consistent with the findings in Zhang et al. (2022b). After ~2060s, their trends vary among different SSPs: under SSP1-2.6, the growth of $CDHD_f$ and $CDHD_s$ are projected to slow down and stagnate, while under SSP2-4.5, SSP3-7.0 and SSP5-8.5, $CDHD_f$ and $CDHD_s$ will keep growing until the end of the century. By 2100, $CDHD_f$ / $CDHD_s$ are projected to increase by 6.5days/0.43, 14.3 days/0.78, 22.2 days/1.21 and 27.5 days/1.43 with reference to 1995-2014 under SSP1-2.6, SSP2-4.5, SSP3-7.0 and SSP5-8.5 respectively. By comparing the increase magnitude of $CDHD_f$ and hot days, we found that the increase of $CDHD_f$ is even faster than the increase of hot days under SSP2-4.5, SSP3-7.0 and SSP5-8.5, indicating that under these 3 SSPs, more and more hot days will occur in the form of CDHD, in other words, accompanied with drought events, thus the portion of CDHD in hot days will increase in the future, which may cause much more severe impacts on wheat production.

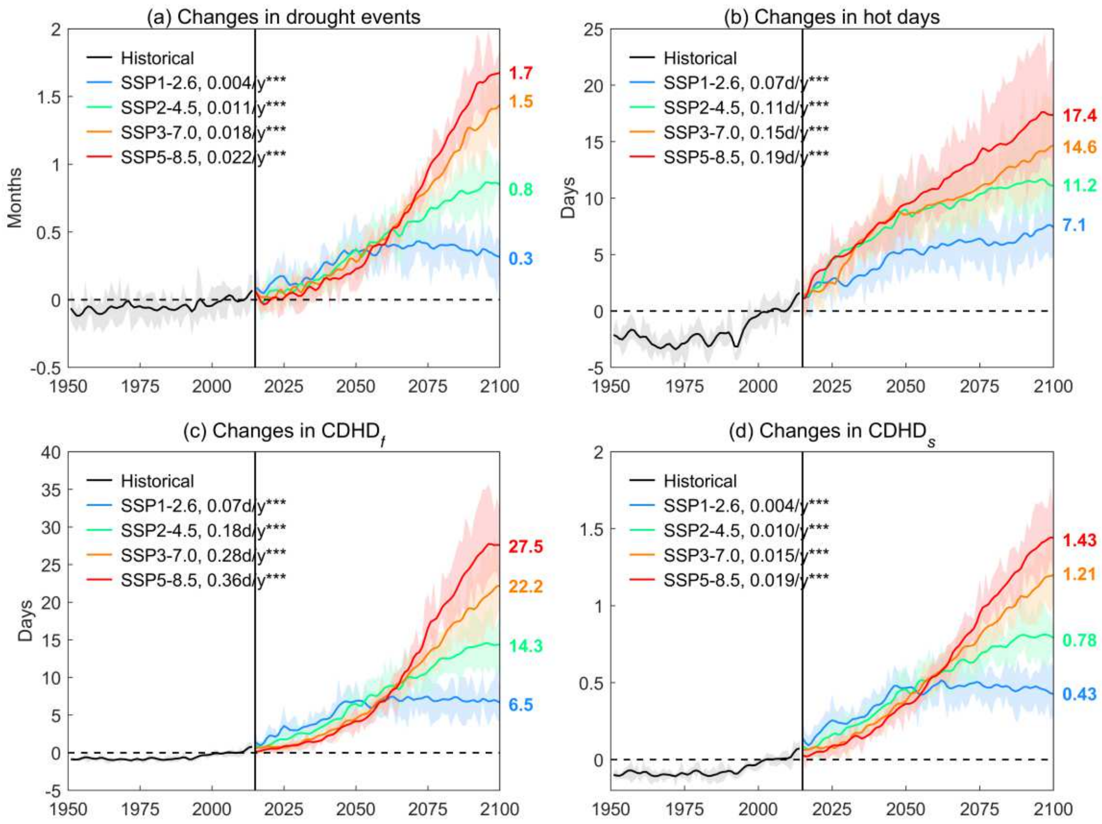

Fig. 2. Global average changes in drought events (a), hot days (b), $CDHD_f$ (c) and $CDHD_s$ (d) for each wheat growing season during 1951-2100 (historical: 1951-2014; future: 2015-2100, under 4 SSPs) with reference to 1995-2014. "***" means the trend is significant at 0.001 level. Solid lines represent 10 GCMs ensemble averages, the top and bottom boundaries of shades represent the 75th and 25th percentiles of 10 GCMs ensemble.

The spatial distributions of the changes in $CDHD_f$ for mid-term future (2041-2060) and long-term future (2081-2100) relative to 1995-2014 are shown in Fig. 3. It is found that $CDHD_f$ will increase over more than 98.6% of wheat planting grids for mid- and long-term under all 4 SSPs. In the mid-term future, the increase of $CDHD_f$ under the 4 SSPs are similar and relatively small, the increment of $CDHD_f$ is less than 10 days in most of wheat planting grids (76.3%-90.0%) under the 4 SSPs. In the long-term future, obvious differences are observed in $CDHD_f$ increment among different SSPs, $CDHD_f$ increment under SSP3-7.0 and SSP5-8.5 is significantly larger than that under SSP1-2.6 and SSP2-4.5. Under SSP1-2.6, $CDHD_f$ increment is less than 10 days in 80.8% of wheat planting grids. Under SSP2-4.5, SSP3-7.0 and SSP5-8.5, $CDHD_f$ increment is larger than 10 days in 40.1%, 49.5% and 58.0% of wheat planting grids, respectively. From spatial heterogeneity, India has the largest $CDHD_f$ increment, whose average $CDHD_f$ increment reaches 59 days in the long-term future under SSP5-8.5. In addition, the increases of $CDHD_f$ over central Africa, Australia, southern Canada, northern America, Ukraine and northern Kazakhstan are much more significant, especially under SSP3-7.0 and SSP5-8.5.

Changes of $CDHD_f$ are determined by the changes of drought events and hot days, the increase of drought events and hot days will positively promote $CDHD_f$ to increase. Fig. S9 and Fig. S10 show the spatial distributions of the changes in drought events and hot days for the mid-term future (2041-2060) and long-term future (2081-2100) under the 4 SSPs, we find that $CDHD_f$ will increase more sharply in the regions where both drought events and hot days are expected to increase substantially. India is the most typical region with both larger increment of drought events and hot days, thus its $CDHD_f$ increment is larger than other regions.

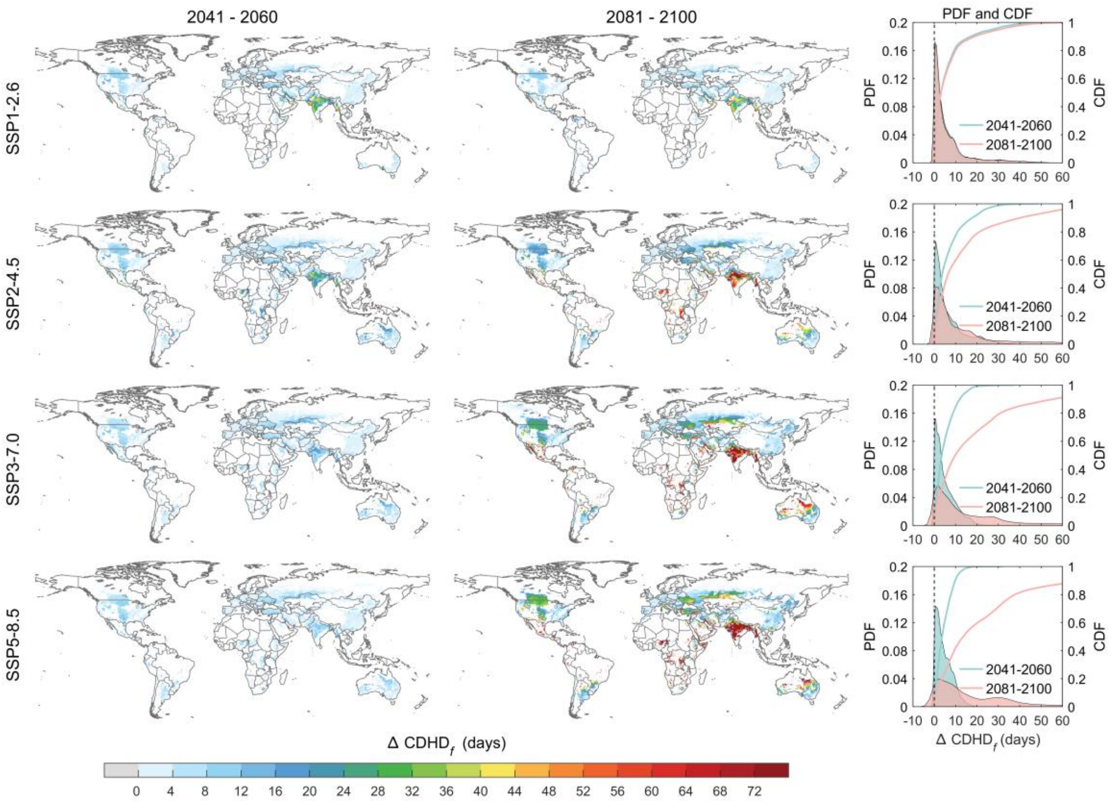

Fig. 3. Spatial distribution, probability density function (PDF) and cumulative distribution function (CDF) of the changes in $CDHD_f$ for mid-term future (2041-2060, the left column) and long-term future (2081-2100, the right column) with reference to 1995-2014 under SSP1-2.6, SSP2-4.5, SSP3-7.0 and SSP5-8.5.

Fig. 4 shows the spatial distribution of changes in $CDHD_s$ for mid-term future and long-term future relative to 1995-2014 under the 4 SSPs. Similar with the changes in $CDHD_f$, $CDHD_s$ is expected to increase over 98.7% of wheat planting grids for mid- and long-term under all 4 SSPs. In the mid-term future, the increase of $CDHD_s$ under the 4 SSPs are similar and relatively small, $CDHD_s$ increment is less than 1 in more than 94.2% of wheat planting grids under the 4 SSPs. In the long-term future, $CDHD_s$ increments under different SSPs are quite different: $CDHD_s$ will increase more sharply under SSP5-8.5, followed by SSP3-7.0, SSP2-4.5 and SSP1-2.6. Under SSP1-2.6, there is no obvious changes in $CDHD_s$ from mid- to long-term future. Under SSP2-4.5, SSP3-7.0 and SSP5-8.5, $CDHD_s$ will increase significantly after mid-term future, $CDHD_s$ increment is larger than 1 in 27.1%, 58.1% and 70.3% respectively. From spatial heterogeneity, India has the largest $CDHD_s$ increment, in addition, $CDHD_s$ will increase more significantly over Turkey, Ukraine, southern Canada, northern America and northern Kazakhstan, especially under SSP3-7.0 and SSP5-8.5.

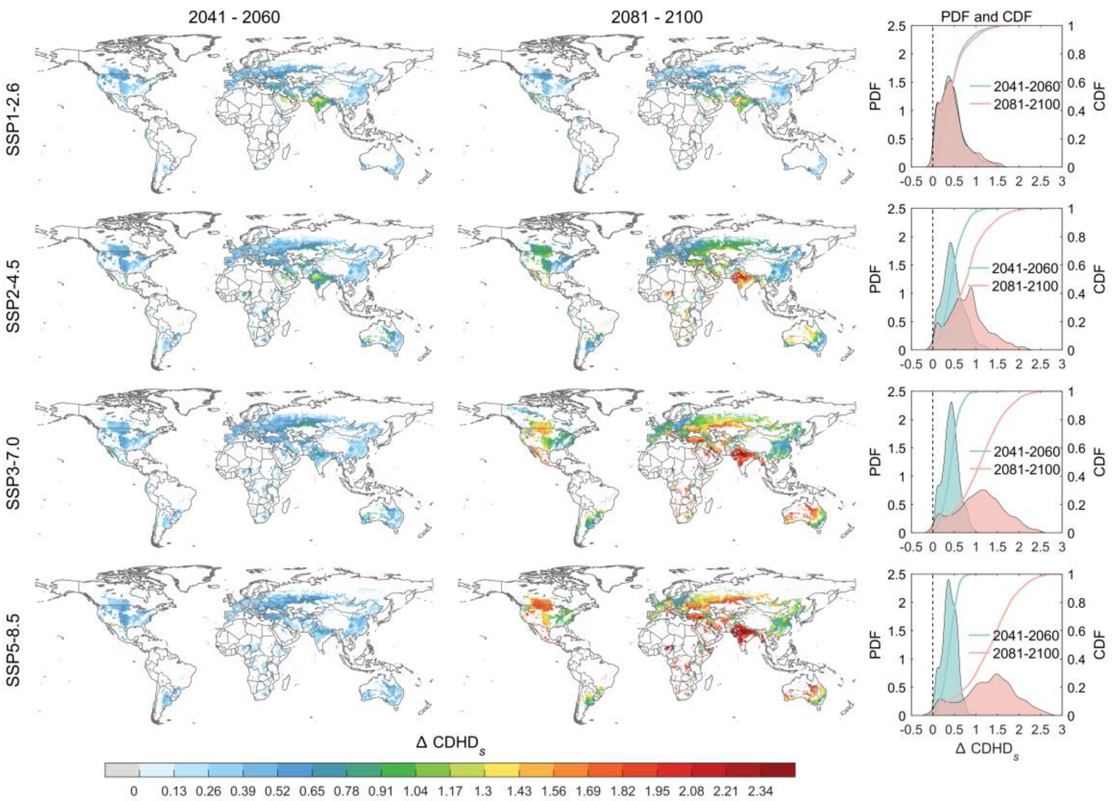

Fig. 4. As Fig. 3 but for $CDHD_s$.

Given the obvious differences in $CDHD_f$ and $CDHD_s$ among different SSPs in the long-term future (2081-2100), we calculate the difference value (D-value) that $CDHD_f/CDHD_s$ in the long-term future under SSP2-4.5, SSP3-7.0, SSP5-8.5 minus that under SSP1-2.6, to investigate what differences will happen in CDHD if adopting low forcing pathway (SSP1-2.6) in the future. As shown in Fig. 5, if adopting low forcing pathway, $CDHD_f/CDHD_s$ will be reduced in 88.7%/91.6%, 92.0%/94.1%, 92.8%/95.1% of wheat planting grids comparing with SSP2-4.5, SSP3-7.0, SSP5-8.5 respectively, in other words, adopting low forcing pathway can mitigate CDHD risks in at least 88.7% of wheat planting grids. It is found that the higher forcing level corresponding to larger D-value of $CDHD_f$ and $CDHD_s$, highlighting the importance of controlling the greenhouse gas emissions to alleviate CDHD risks. $CDHD_f$ and $CDHD_s$ over India, Turkey, Canada and America will respond more strongly to the forcing level increasing, in other words, more sensitive to forcing level increasing. Therefore, they will benefit the most if adopting low forcing pathway in the future.

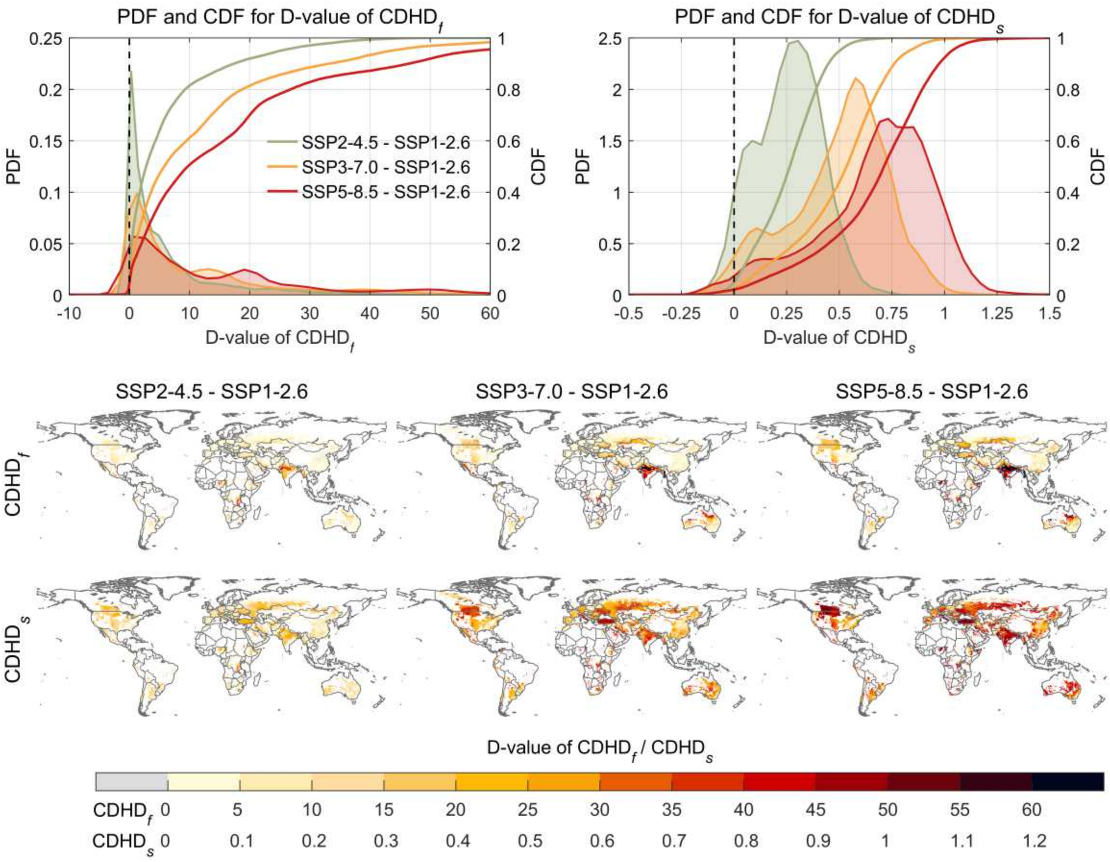

Fig. 5. The probability density function (PDF), cumulative distribution function (CDF) and spatial distribution of the difference value (D-value) of $CDHD_f$ and $CDHD_s$ for the long-term future (2081-2100) between SSP2-4.5 and SSP1-2.6, between SSP3-7.0 and SSP1-2.6,

between SSP5-8.5 and SSP1-2.6.

3.2 CDHD in the key wheat producers

Given the large spatial heterogeneity existing in both wheat production and CDHD, CDHD occurring in the key wheat producers may lead to larger risks to global food security, thus more attention should be paid to the changes of CDHD in these regions. In this section, we focus on the top 10 wheat producing countries with the largest wheat production in 2020: China, India, Russia, America, Canada, France, Pakistan, Ukraine, Germany and Turkey, their wheat production and planting area reach up to 535.6 Mt and 138.1 Mha in 2020, accounting for 70.4% and 63.1% of the global total (wheat production and planting area of each country are shown in Table S1). Here we compare the $CDHD_f$ and $CDHD_s$ of the top 10 countries for mid- and long-term future under the 4 SSPs (detailed values are shown in Table S2-S3), to explore who will be the hotspots that will suffering more potential risks from CDHD.

As Fig. 6 shows, a consistent finding is, in the mid-term future, $CDHD_f$ under SSP1-2.6 is the largest, followed by SSP2-4.5, SSP3-7.0 and SSP5-8.5, the differences of $CDHD_f$ among the 4 SSPs are relatively mild. While in the long-term future, $CDHD_f$ under SSP5-8.5 is the largest, followed by SSP3-7.0, SSP2-4.5 and SSP1-2.6, the differences of $CDHD_f$ among the 4 SSPs are more pronounced than that in the mid-term future, indicating that CDHD will be more substantially promoted after mid-term future, thereby aggressive adaptation strategies should be taken as soon as possible. By comparing the $CDHD_f$ (the median of GCMs ensemble) of the 10 countries, India, Ukraine, Turkey and America will suffer more CDHD in wheat growing seasons in both mid- and long-term future under all SSPs. Conversely, France, Germany and China will suffer less CDHD in wheat growing seasons in both mid- and long-term future under all SSPs.

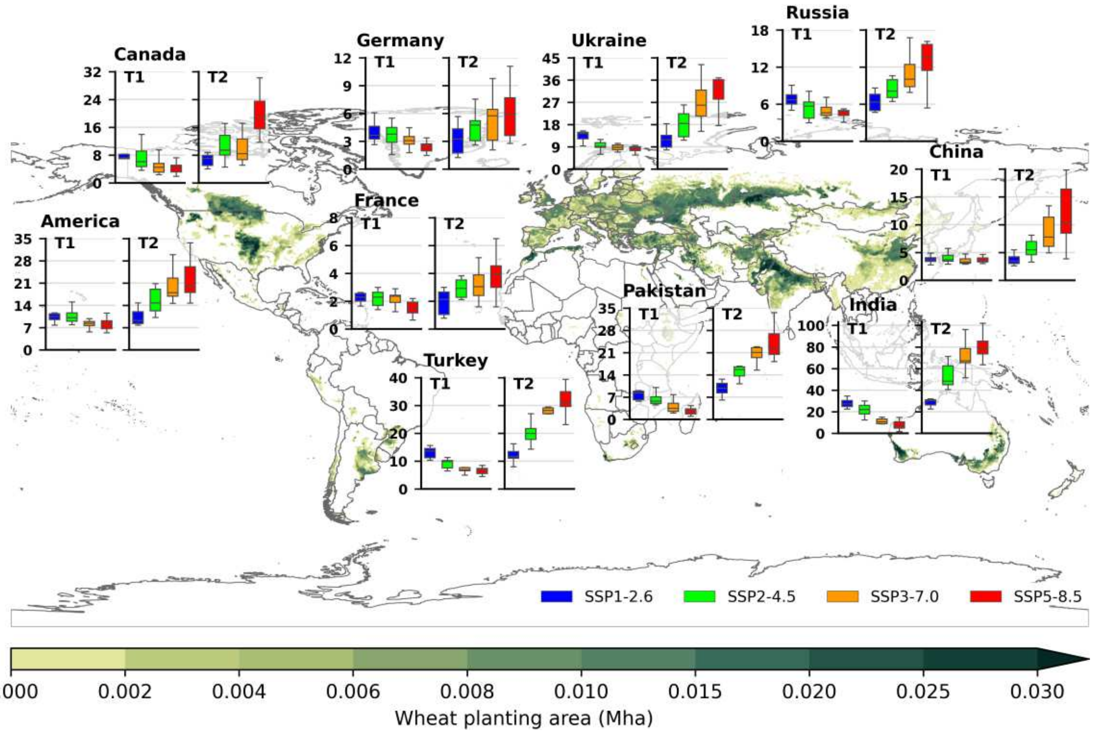

Fig. 6. Projected $CDHD_f$ (days) of the top 10 wheat producing countries for mid-term future (2041-2060, T1) and long-term future (2081-2100, T2) under 4 SSPs. The boxplots display the spread of $CDHD_f$ projected by 10 GCMs that represent uncertainties of GCMs ensemble, the background is the spatial distribution of wheat planting area in 2020.

As Fig. 7 shows, similarly with $CDHD_f$, in the mid-term future, $CDHD_s$ under SSP1-2.6 is the largest, followed by SSP2-4.5, SSP3-7.0 and SSP5-8.5; while in the long-term future, $CDHD_s$ under SSP5-8.5 is the largest, followed by SSP3-7.0, SSP2-4.5 and SSP1-2.6, the differences of $CDHD_s$ among the 4 SSPs are more pronounced than that in the mid-term future. By comparing the $CDHD_s$ (the median of GCMs ensemble) of the 10 countries, it is found that wheat in India, Ukraine, Turkey, Russia and America will suffer more severe CDHD in wheat growing seasons. Conversely, $CDHD_s$ in France, Pakistan, Canada, China and Germany are relatively smaller than other top 10 countries.

By comparing $CDHD_f$ and $CDHD_s$ of the top 10 countries, it is found that $CDHD_f$ and $CDHD_s$ of Ukraine, Turkey and America are among the top 5 in both mid- and long-term future under all SSPs, indicating that Ukraine, Turkey and America will be the hot spots that will suffer much more and stronger CDHD in future wheat growing seasons.

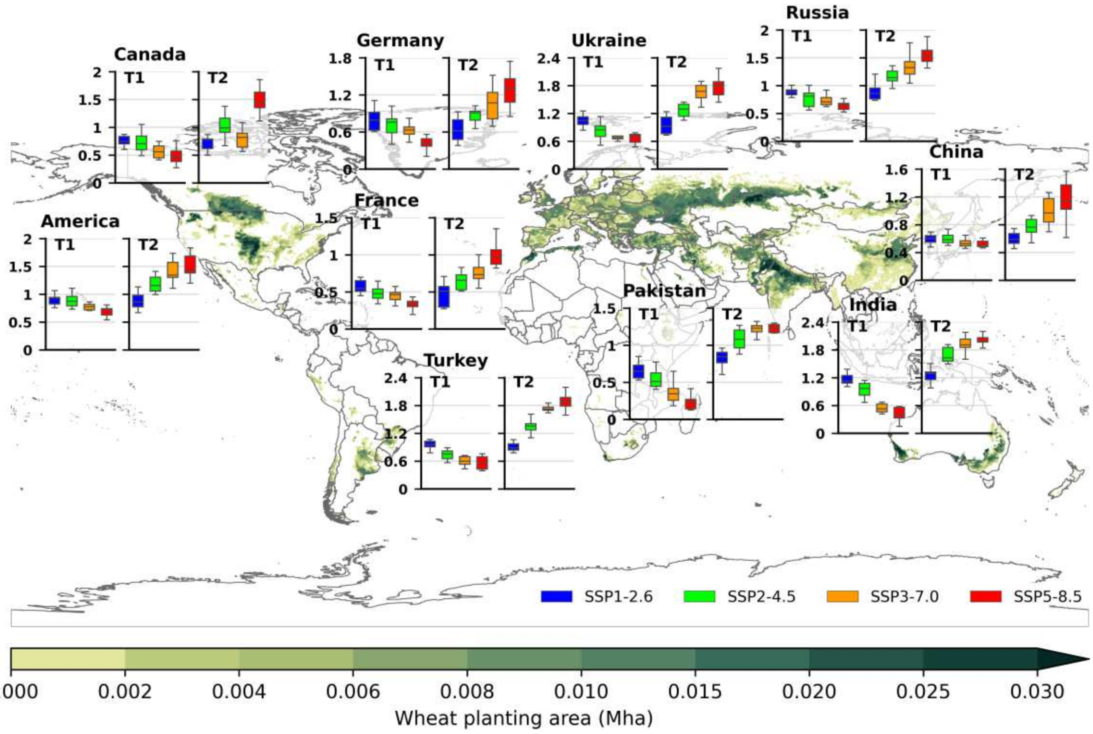

Fig. 7. As Fig. 6 but for $CDHD_S$.

3.3 Global warming will dominate the increase of CDHD

In this study, drought events are identified as SPEI≤-1 because SPEI has higher correlation with crops yield compared with other drought indices such as SPI and PDSI (Tian et al., 2018). Here we should note that SPEI is highly correlated with temperature, which is produced by standardizing the difference between precipitation and potential evapotranspiration (PET, calculated based on temperature, as shown in Eq. 6-8), thus it is also already an indicator of compound drought and heat conditions to some extent (Vogel et al., 2021). Therefore, the change in drought events in this study is determined by both precipitation and temperature. In order to clarify who will dominate the increase of CDHD in the future, we calculated the global average PET of each wheat growing season during 2015-2100 under the 4 SSPs to explore how will PET change under global warming. Furthermore, we also identified drought events and CDHD within wheat growing seasons based on SPI≤-1. SPI is calculated similarly to SPEI but only based on precipitation, while SPEI is calculated based on the difference between precipitation and PET, thus we can explore the impacts of PET (or temperature) on drought events and CDHD by comparing the results based on SPI and SPEI, as shown in Fig. 8.

As shown in the left column of Fig. 8, the average PET in wheat growing season is projected to increase significantly during 2015-2100 by 0.08mm/y, 0.20mm/y, 0.29mm/y and 0.46mm/y under SSP1-2.6, SSP2-4.5, SSP3-7.0 and SSP5-8.5 respectively, indicating that PET will be promoted significantly by temperature rising in the future. As shown in the middle column of Fig. 8, obvious differences can be observed between SPI-based drought events and SPEI-based drought events, such differences will expand alongside with temperature rising until the end of the century. By 2100, the differences between SPEI-based drought events and SPI-based drought events will increase to 0.7 month, 1.2 months, 1.8 months and 2.1 months under SSP1-2.6, SSP2-4.5, SSP3-7.0 and SSP5-8.5 respectively. SPI-based drought events will slightly but significantly decrease under all SSPs, indicating that precipitation within wheat growing seasons is projected to increase. SPEI-based drought events will increase significantly under all SSPs, indicating that the difference between precipitation and PET will decrease, considering that precipitation will increase as analyzed above, we can draw the conclusion that the substantial increase of PET alongside with global warming is the decisive factor of drought events' growth rather than precipitation deficits, in other words, global warming will dominate the increase of drought events via substantially promoting PET to growth.

The global average SPI-based $CDHD_f$ and SPEI-based $CDHD_f$ within wheat growing seasons of 2015-2100 under the 4 SSPs are shown in the right column of Fig. 8. Obvious differences are observed between SPI-based $CDHD_f$ and SPEI-based $CDHD_f$, such differences are projected to expand over the future, which could be attributed to the differences between drought events based on SPI and SPEI. By 2100, SPEI-based $CDHD_f$ are 6.6 days, 12.2days, 18.4 days and 28.6 days greater than SPI-based $CDHD_f$ under SSP1-2.6, SSP2-4.5, SSP3-7.0 and SSP5-8.5 respectively. SPI-based $CDHD_f$ will increase slightly but significantly under SSP2-4.5, SSP3-7.0 and SSP5-8.5, considering that SPI-based drought events will decrease significantly, thus the increase of SPI-based $CDHD_f$ is attributed to the increase of hot days. SPEI-based $CDHD_f$ will increase significantly under all SSPs, which is attributed to the increase of both drought events and hot days. From the analysis above, we have known that the increase of SPEI-based drought events is attributed to the increase of PET caused by temperature rising, therefore we can draw the conclusion that global warming will determine the increase of SPEI-based $CDHD_f$, which via two pathways: on the one hand, temperature rising will substantially promote PET thereby causing significant increase in drought events;

on the other hand, temperature rising will directly promote hot days to increase.

Consistent conclusions can be found in previous studies. Sarhadi et al. (2018) proved that the increasing trends in warm year probability can substantially promote the increase of compound warm and dry year probability. Yu et al. (2020) demonstrated that the increase of hot extremes under global warming is the major driver of the increase of compound drought and hot extremes since the late 1990s in eastern China. Zhang et al. (2022b) proved that temperature is the dominant factor influencing compound drought and hot extremes by using path analysis. Our study further reveals that global warming will dominate the future increase of CDHD via directly promote hot days and indirectly promote PET to aggravate droughts, pointing out the importance and urgency of adopting adaptive measures for responding global warming.

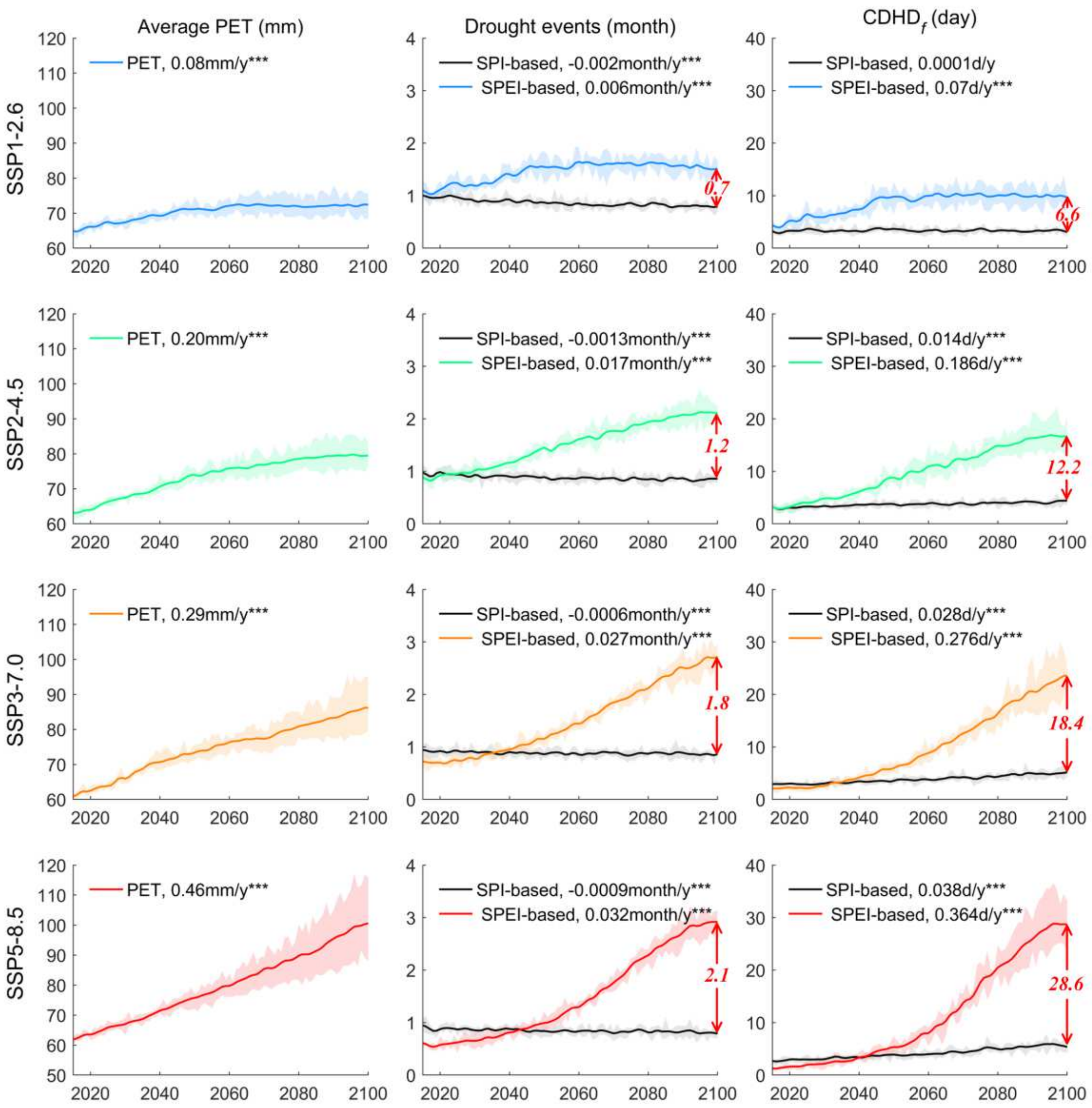

Fig. 8. Global average changes in PET (a), SPI- and SPEI-based drought events (b), SPI- and SPEI-based $CDHD_f$ (c) in wheat growing season during 2015-2100 under SSP1-2.6, SSP2-

4.5, SSP3-7.0 and SSP5-8.5. "***" means the trend is significant at 0.001 level. Solid lines represent 10 GCMs ensemble averages, the top and bottom boundaries of shades represent the 75th and 25th percentiles of 10 GCMs ensemble.

In order to investigate the spatial heterogeneity of the impacts of global warming on drought events and CDHD identification, we display the spatial distributions of the differences between SPEI-based drought events and SPI-based drought events, and between SPEI-based $CDHD_f$ and SPI-based $CDHD_f$ for the long-term future (2081-2100) under 4 SSPs, as shown in Fig. 9. From the left column of the Fig. 9, it is found that by the end of the century, SPEI-based drought events will be greater than SPI-based drought events in 97.6%~100.0% of wheat planting grids, especially over India, Pakistan, Myanmar, Iran, central China and central Australia, indicating that SPEI droughts will increase more substantially than SPI droughts over the world's wheat planting regions under global warming, SPI will underestimate drought conditions especially under high forcing scenarios where increased PET becomes the driver of droughts but not precipitation. From the right column, SPEI-based CDHD will be greater than SPI-based CDHD over 98.8%~99.3% of wheat planting grids by the end of the century, such difference is more substantial over India, Myanmar and central Australia. These results show the great impacts of PET promoted by global warming on drought events and CDHD in the future, indicating the dominance of global warming in promoting droughts and CDHD worldwide, especially under high forcing scenarios. Also, it is proved that drought indices solely based on precipitation (such as SPI) cannot reveal warming-induced changes in droughts thus they will underestimate drought component thereby underestimate CDHD.

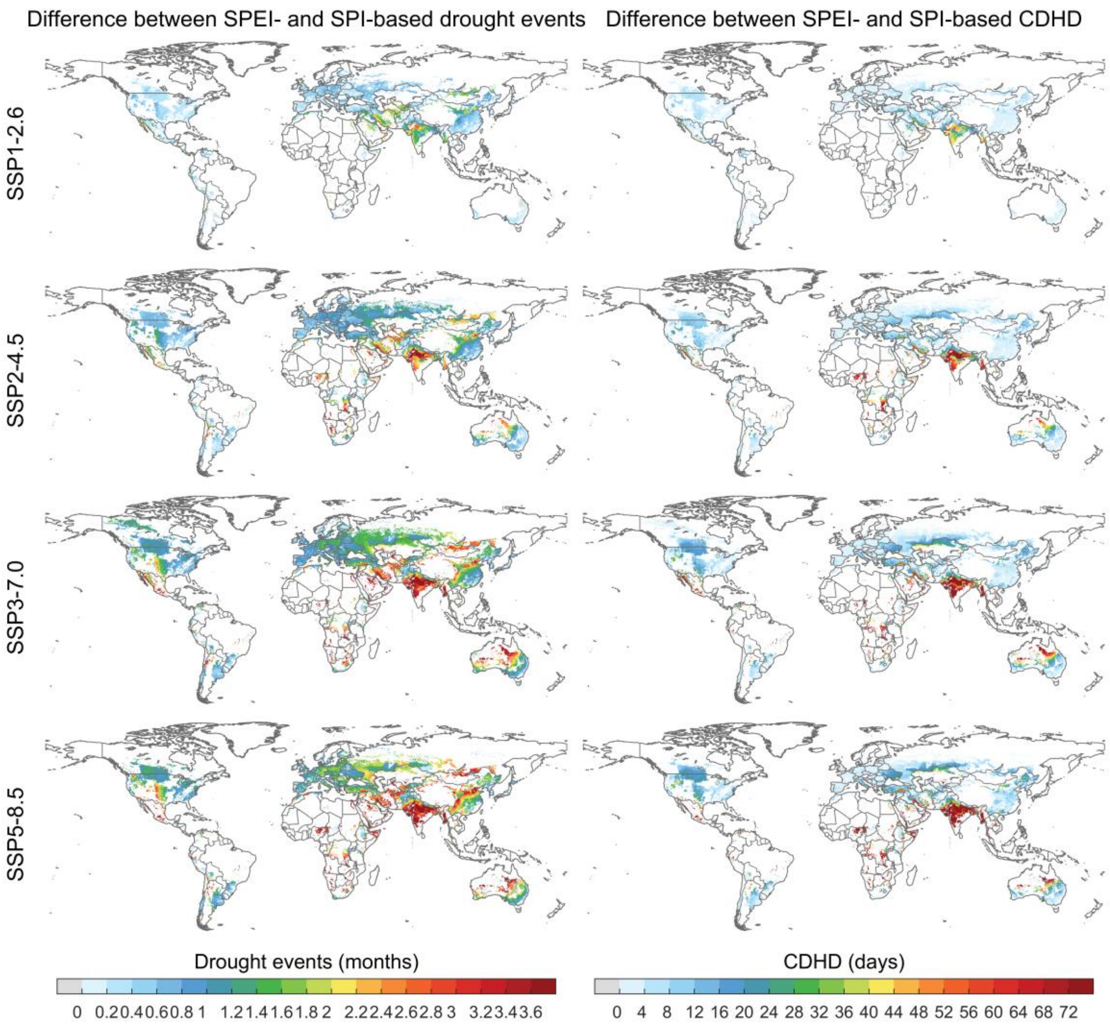

Fig. 9. Spatial distributions of the differences between SPEI-based drought events and SPI-based drought events (the left column), and the difference between SPEI-based CDHD and SPI-based CDHD (the right column) for wheat growing seasons of the long-term future (2081-2100) under SSP1-2.6, SSP2-4.5, SSP3-7.0 and SSP5-8.5.

4 Discussion

4.1 Correlations between drought events, hot days and CDHD

From the analysis above, we have known that global warming will dominate future increase in CDHD within wheat growing seasons via increasing PET to promote drought events and via increasing hot days directly. Here we calculated the Pearson correlation coefficient (r) to investigate the link between the changes in drought events (Δ drought events) and CDHD ($\Delta CDHD_f$), and between the changes in hot days (Δ hot days) and CDHD ($\Delta CDHD_f$), respectively, for the long-term future (2081-2100) relative to 1995-2014 under the 4 SSPs, as shown in Fig. 10.

As shown in Fig. 10, positive and significant correlations are found between Δ drought events and $\Delta CDHD_f$, and between Δ hot days and $\Delta CDHD_f$ under all SSPs, Pearson correlation coefficients between Δ drought events and $\Delta CDHD_f$ are 0.71~0.76, Pearson correlation coefficients between Δ hot days and $\Delta CDHD_f$ are 0.43~0.53, indicating that the increase of both drought events and hot days will make positive contributions to the increase of CDHD in the future. Pearson correlation coefficients between Δ drought events and $\Delta CDHD_f$ are always greater than that between Δ hot days and $\Delta CDHD_f$ under all SSPs, in other words, Δ drought events are more closely correlated with $\Delta CDHD_f$, indicating that the increase of drought events that mainly driven by substantial growth of PET is presumably the main contributor to the increase of CDHD, besides, the increase of hot days directly caused by global warming will also positively promote CDHD to growth in future wheat growing seasons.

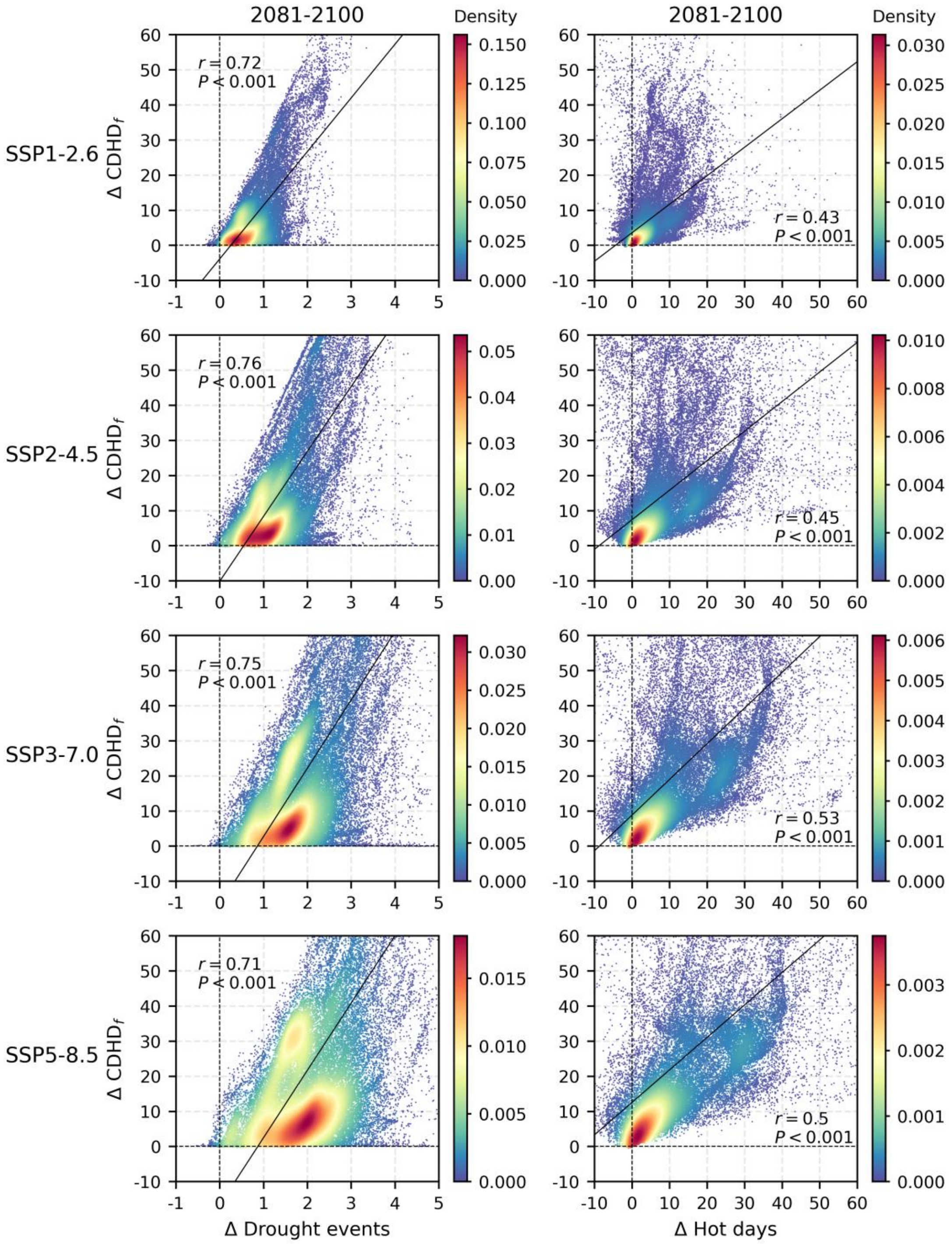

Fig. 10. The density of wheat planting grids with different changes in drought events and $CDHD_f$ (left column), different changes in hot days and $CDHD_f$ (right column) for 2081-2100 relative to 1995-2014 under the 4 SSPs, and their Pearson correlation coefficient (r) and significance level (P).

4.2 Uncertainties

Our results are subjected to some uncertainties induced by CMIP6 models simulations, wheat planting regions projection, wheat growing season projection and the selection of drought and heat indices. 1) Although we use 10 GCMs ensemble averages to reduce uncertainties in future climate variables projection as much as possible, we still need to pay attention to the uncertainties from GCMs simulations, especially in long-term future. 2) The temporal resolution of the wheat planting regions projection used in this study is 5 years, therefore, we assume that the wheat planting regions remain the same in each 5-year period, which could have brought uncertainties into results. 3) The change in crop growing season is affected by both climate and anthropogenic factors (adjusting sowing date, using improved cultivar, etc.). In the projection of wheat growing season in this study, we focus on the impacts of climate change, thus we assume that the planting dates and cultivar selection remain unchanged, the length of wheat growing season is determined by the required time for heat accumulation reaching the total heat requirement. Such projections do not consider the impacts from the development of agricultural management strategies on wheat growing season, which could have brought uncertainties into results. It is mainly due to the absence of a comprehensive, scientific and continuous predictions for wheat growing season that considering impacts of both climate change and technological development. 4) Agricultural drought is a comprehensive phenomenon that comprising precipitation shortages, evapotranspiration reduction and soil moisture deficits (Łabędzki et al., 2015). We use SPEI to capture drought events in wheat growing season, which containing the impacts of both precipitation and temperature (via affecting potential evapotranspiration). SPEI is proved to be the most representative of soil moisture conditions and has higher correlation with crops yield (Tian et al., 2018). As this study is a global- scale research, we use a consistent heat threshold (daily maximum temperature greater than 30°C) following previous studies (Chen et al., 2016). In further research, we would like to explore the impacts of using different heat thresholds for different wheat growing stages and for different wheat planting regions on CDHD.

5 Conclusion

This study provides a comprehensive analysis of the changes in compound dry and hot days (CDHD) occurring within dynamic wheat growing seasons of 2015-2100 under SSP1-2.6, SSP2-4.5, SSP3-7.0 and SSP5-8.5 over global wheat planting regions, including their frequency ($CDHD_f$) and severity ($CDHD_s$). This study sought to fill the gap in knowledge by identifying the CDHD occurring within dynamic crops growing seasons, and clarifying the driven mechanism of global warming to CDHD increase. The main findings are summarized as follows.

Under global warming, global average length of winter/spring wheat growing season will be shorten by 9days/5days, 20 days/16days, 34 days/26 days and 49 days/29 days in 2100 under SSP1-2.6, SSP2-4.5, SSP3-7.0 and SSP5-8.5, respectively. The reduction of wheat growing days over Europe, southern China and central America are much more significant, especially under SSP3-7.0 and SSP5-8.5.

CMIP6 multi-GCMs ensemble project a substantial increasing trend in global average $CDHD_f$ and $CDHD_s$ under all SSPs. By 2100, $CDHD_f/CDHD_s$ are projected to increase by 6.5days/0.43, 14.3 days/0.78, 22.2 days/1.21 and 27.5 days/1.43 with reference to 1995-2014 under SSP1-2.6, SSP2-4.5, SSP3-7.0 and SSP5-8.5 respectively. $CDHD_f$ / $CDHD_s$ will increase more sharply over India, southern Canada, northern America, Ukraine and northern Kazakhstan. Higher forcing level corresponds higher $CDHD_f$ and $CDHD_s$, adopting low forcing pathway (SSP1-2.6) can reduce $CDHD_f$ and $CDHD_s$ in 88.7%-92.8% and 91.6%-95.1% of wheat planting grids. As the top 10 wheat producers, Ukraine, Turkey and America will be the hot spots that will suffer much more and stronger CDHD in future wheat growing seasons.

Potential evapotranspiration (PET) within wheat growing season is projected to increase substantially driven by global warming especially under high forcing pathways, thus drought events will be dominated by global warming rather than precipitation deficits. Drought indices solely based on precipitation (such as SPI) cannot reveal warming-induced changes in droughts thus they will underestimate drought component thereby underestimate CDHD. Global warming will dominate the increase of CDHD within wheat growing seasons in the future directly by promoting hot days to increase and indirectly by enhancing PET thereby promoting drought events.

This study provides an analysis framework for investigating future variations of compound extremes occurring in dynamic crops growing seasons worldwide. Our results reveal the future changes of CDHD, the most threatening climatic stress for wheat, during dynamic wheat growing seasons of 2015-2100 under different socio-economic scenarios, improve the understanding of how global warming will impact CDHD's increase, and highlight the importance and urgency of implementing adaptation measures to response CDHD risks for safeguarding wheat production and food security.

Supplementary Files

This is a list of supplementary files associated with this preprint. Click to download.

- References.docx
- Declaration.docx
- SupportingInformation.docx